To cite this article: LI W, WANG Y, NING J, et al. Unmanned ship heading tracking control strategy with state quantization and input quantization [J/OL]. Chinese Journal of Ship Research, 2024, 19(1). http://www.ship-research.com/en/article/doi/10.19693/j.issn.1673-3185.03318 (in both Chinese and English).

DOI: 10.19693/j.issn.1673-3185. 03318

Unmanned ship heading tracking control strategy with state quantization and input quantization

LI Wei[1], *WANG Yu*[1], *NING Jun*[*1], *LI Zhihui*[2]

1 Navigation College, Dalian Maritime University, Dalian 116026, China

2 College of Information Technology, Jilin Normal University, Siping 136000, China

Abstract: [**Objective**] This paper develops a heading tracking design strategy for unmanned surface vessels (USVs) with state quantization and input quantization in order to address the problem of limited communication at sea for unmanned ships on the water surface. [**Methods**] First, a control law is designed on the basis of backstepping and combined with dynamic surface control to reduce the computational complexity of the virtual control law. An extended state observer (ESO) is also designed to estimate uncertainties and unknown disturbances. Second, all state variables and control variables in the control system are assumed to be quantized by the uniform quantizer, and the quantized state feedback information is only available for the tracking control design. A controller of USVs based on the ESO and using quantized states is recursively designed to ensure the tracking of the desired heading. The boundedness of the quantization errors between quantized variables and non-quantized variables in the closed-loop system is analyzed by presenting several theoretical lemmas. [**Results**] Based on the Lyapunov stability theory, the stability of the designed unmanned ship heading tracking control system with state quantization and input quantization is demonstrated, and the simulation results verify the effectiveness of the resulting tracking scheme. [**Conclusion**] The results of this study can provide references for the heading tracking of unmanned ships.

Key words: unmanned surface vessels; state quantization and input quantization; quantitative feedback control; extended state observer; quantization error

CLC number: U664.82

0 Introduction

With the rapid development of intelligent navigation technology, unmanned surface vessels (USVs) have received widespread attention. This intelligent unmanned marine transportation platform, which sails remotely or autonomously, is valuable for research because it can take into account safety and economy while conducting marine operations in a complex marine environment.

As one of the key technologies of USV, heading control has been the focus and hot spot of research in the field [1-3]. To obtain the good heading tracking control effect, Wu et al. [4] applied neural network algorithm to parameter identification in the heading control of ships. Ma et al. [5] combined radial basis function (RBF) neural network and PID control algorithm, and put forward a heading automatic control method for ship based on the prediction of RBF neural network, which improves the control accuracy. An et al. [6] converted the state vector of the system into an error variable and linearized it, and then proposed an adaptive controller based on backstepping according to the idea of reverse recursion and the feedback linearization theory, which overcomes the nonlinearity and uncertainty of the motion model of ships. Han [7] combined a neural network and fuzzy logic, and put forward the adaptive fuzzy neural network control method to adapt to the disturbances of the high sea state, which ensures the rapidity and stability of the control system. Li et al. [8] proposed an adaptive control method based on event-triggered ship heading logic switching on the basis of the combination of a

Received: 2023－04－10 **Accepted:** 2023－06－15

***Corresponding author:** NING Jun

neural network and fuzzy logic, which effectively reduces the update frequency of control signals. It is worth noting that most of the above studies only considered how to enhance the control accuracy [9], stability, robustness[10], etc. of ship heading tracking. However, in nautical practice, the control signals need to be transmitted through communication channels. Due to the limited communication bandwidth at sea, it is of more nautical significance to consider ship heading tracking control with input quantization and state quantization to ensure that the system operates properly within a given bandwidth.

Quantization is a process of converting continuous signals into a set of discrete symbols or integer values. In the heading control system of a ship, the active quantization of the control input can not only reduce the burden of signal transmission, reduce the rudder execution frequency, but also the rudder amplitude, which is more in line with the control law of the rudder servo system in nautical practice. However, a process of quantizing the system signals makes an approximation of data. Therefore, a quantization error inevitably arises, and that error may accumulate over time. When the error is too large, it may lead to a degradation of tracking performance and a decrease in the stability of the control system. Therefore, the analysis of quantification errors is particularly important.

Research on quantitative feedback control and quantization of errors has received much attention. Regarding the nonlinear system with strict feedback and input quantization, Zhou et al. [11] investigated a hysteresis quantizer and proposed an adaptive tracking control method based on backstepping. Liu[12] extended the applicability of adaptive tracking control to high-order nonlinear systems by adding a homogeneous control algorithm to the control design. Qi et al. [13] added the dynamic surface control technology to further propose an adaptive fuzzy control method. Wu et al. [14] added a positive integrable time-varying function and further proposed an adaptive asymptotic tracking control method. Compared to the input quantization problem, relatively little research has been carried out on the state quantization problem. Regarding the nonlinear system with state quantization, Zhou et al. [15] proposed an adaptive control method based on backstepping. Kim et al.[16] proposed an adaptive quantized feedback tracking control method based on neural networks. Since it is not possible to compute the time derivative of discontinuously quantized state feedback information in Lyapunov's recursive design step, it poses a challenge to the design work of control systems with state quantization. In addition, there is a lack of theoretical research on quantized feedback heading tracking control for USVs with state quantization and input quantization.

Based on the above analysis, in this paper, a quantized feedback heading tracking control method based on extended state observer (ESO) for the USV heading tracking control problem with state quantization and input quantization. Designing the system control laws based on backstepping is combined with dynamic surface technology to reduce the computationally inflated problem of virtual control laws. ESO is utilized to estimate the uncertainty terms and unknown perturbations in the system model. A uniform quantizer is used to quantize the state variables and the control inputs in the control system, respectively, and the quantized state feedback information is used only for tracking control. Stability analysis of a closed-loop feedback control system with quantization error based on Lyapunov's stability theory rigorously demonstrates the closed-loop stability of the designed feedback control system and the boundedness of the quantization errors.

1 System description

The mathematical model of USV heading control can be expressed as [17]

$$\begin{cases} \dot{\psi} = r \\ \dot{r} = a_1 r + a_2 r^3 + b\delta + \omega \\ \tau = \delta \end{cases} \tag{1}$$

where ψ is a ship's heading angle; r is a ship's yaw rate; ω is the unknown perturbation of the system; τ is the control input of the system; δ is a ship's rudder angle; a is the nonlinear coefficient of Norrbin's motion model, $a_1 = -1/T$, $a_2 = -a/T$; b is the gain of the control system, $b = K/T$. K is the spinning exponent of a ship; T is a ship's follow-ability exponent, $T = T_1 + T_2 + T3$, and $T_1 - T_3$ are the followability indices of a ship. (ψ, r) is selected as the state variables. Define $x_1 = \psi$, $x_2 = r = \dot{\psi}$, $f(x,t) = a_1 r + a_2 r^3 + \omega$. Select $\tau = \delta$. $Q(\tau)$ is taken as the quantized control input to a system. According to References [18-19], quantization converts continuous signals into segmented constant signals.

Therefore, the mathematical model of USV heading control after input quantization is introduced:

$$\begin{cases} \dot{x}_1 = x_2 \\ \dot{x}_2 = f(x,t) + bQ(\tau) \end{cases} \tag{2}$$

In this paper, the problem of USV heading tracking control with state/input quantization is considered. The quantization controller receives the quantized state variables from the controlled object-1 via the network system, and then transmits the quantized system control inputs to the controlled object-1 via the network system. The continuous signals are linearly mapped to the nearest shaping value by affine transformation. The floating-point number is scaled, rounded, and undergoes a series of other operations to obtain the result of shaping in a discrete space after quantization, i. e., uniform quantization [17-21]. In this paper, all state variables x_1 and x_2 and control input τ are quantized using a uniform quantizer:

$$Q(s) = \begin{cases} L_i, & L_i - \chi/2 \leqslant s < L_i + \chi/2 \\ 0, & -\chi/2 \leqslant s < \chi/2 \\ -L_i, & -L_i - \chi/2 \leqslant s < -L_i + \chi/2 \end{cases} \tag{3}$$

where s stands for x_1, x_2, and τ, respectively; $\chi > 0$ denotes the quantization step, $L_1 = \chi$, $L_{i+1} = L_i + \chi$, $i \in \mathbf{R}$. After quantization, the state variable and the input variable s become $Q(s)$. This process generates a quantization error. From Reference [21], it is known that the quantization error $s - Q(s)$ satisfies $|s-Q(s)| \leqslant \chi$.

The control objective of this paper is to design the quantized feedback tracking control law τ based on ESO, so that the heading angle x_1 of the system can track the desired heading $x_{1\mathrm{d}}$. The yaw rate x_2 of the system can track the desired yaw rate $x_{2\mathrm{d}} = \dot{x}_{1\mathrm{d}}$.

Hypothesis 1 [22]: The quantized state variables $Q(x_1)$ and $Q(x_2)$ can be used to design the control input τ of the system.

Hypothesis 2: The uncertainty term $f(x, t)$ is an unknown continuous function whose time derivative exists and is bounded.

Regarding the quantized feedback control problem, Hypothesis 1 is proposed, i.e., the controller is designed using only the quantized heading angle and the yaw rate. Hypothesis 2 means that the proposed quantized feedback controller is designed without a prior information about the uncertainties of the system and external disturbances. By utilizing ESO, the observation of the unknown term is achieved and the uncertainty of the model can be overcome.

2 Quantized feedback tracking controller design

In this paper, an ESO-based quantized feedback tracking control method is designed for the motion model of USVs (as shown by Eq. (2)) with state quantization and input quantization, and the control structure is shown in Fig. 1. After quantizing the state variables of Eq. (2), the quantized state variables are transmitted to the controller through the network, and then the system control inputs are obtained. The control inputs are then quantized. The quantized control inputs are transmitted to the controlled object-1 via the network. The main objective of this chapter is to design the ESO-based quantized feedback tracking controller.

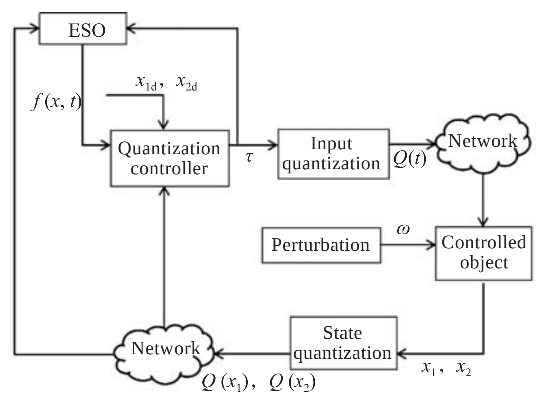

Fig. 1 Simplified block diagram of quantitative feedback tracking control system based on ESO

2.1 ESO-based quantized feedback controller design

The error surface is defined as

$$\eta_1 = x_1 - x_{1\mathrm{d}} \tag{4}$$

$$\eta_2 = x_2 - \alpha \tag{5}$$

where $x_{1\mathrm{d}}$ is the desired heading signal; α is the filtered signal of the virtual signal $\bar{x}_2$.

A first-order low-pass filter is selected as

$$\begin{cases} \varsigma\dot{\alpha} + \alpha = \bar{x}_2 \\ \alpha(0) = \bar{x}_2(0) \end{cases} \tag{6}$$

where ς is the filtering parameter of the first-order low-pass filter and is a positive constant.

The design steps of the ESO-based quantized feedback tracking controller proposed in this paper are as follows: designing the virtual signal $\bar{x}_2$ of the state variable x_2 to ensure the convergence of the heading error η_1; then passing the virtual signal $\bar{x}_2$ through the low-pass filter(as shown by Eq. (6)) to obtain the filtered signal α. The unknown terms of the system are observed with the ESO. The control input $\bar{\tau}$ is designed using the quantized state variables to ensure that the velocity error converges as follows.

Step 1: Deriving the error surface Eq. (4) to obtain

$$\dot{\eta}_1 = \dot{x}_1 - \dot{x}_{1d} = x_2 - \dot{x}_{1d} \tag{7}$$

The virtual signal $\bar{x}_2$ is selected as

$$\bar{x}_2 = -c_1\eta_1 + \dot{x}_{1d} \tag{8}$$

where c_1 is the normal number.

In the inverse design, if $\alpha = -c_1\eta_1 + \dot{x}_{1d}$ is used, it will lead to the time-differential explosion when $\dot{\alpha}$ is solved. Based on the dynamic surface technology, the low-pass filter α will be obtained by inputting $\bar{x}_2$ into the first-order low-pass filter. The following can be obtained from Eq. (6):

$$\dot{\alpha} = \frac{\bar{x}_2 - \alpha}{\varsigma} \tag{9}$$

Step 2: Deriving the error surface Eq. (5) to obtain the following:

$$\dot{\eta}_2 = \dot{x}_2 - \dot{\alpha} = bQ(\tau) + f - \dot{\alpha} \tag{10}$$

where f is the unknown term whose time derivative exists and is bounded, and is estimated using ESO.

The ESO is designed as

$$\begin{cases} \dot{\hat{x}}_1 = \hat{x}_2 + 3(x_1 - \hat{x}_1)/\varepsilon \\ \dot{\hat{x}}_2 = \hat{\sigma} + b\bar{\tau} + 3(x_1 - \hat{x}_1)/\varepsilon^2 \\ \dot{\hat{\sigma}} = (x_1 - \hat{x}_1)/\varepsilon^3 \end{cases} \tag{11}$$

By using this expansion observer, it is possible to realize $\hat{x}_1(t) \to x_1(t)$, $\hat{x}_2(t) \to x_2(t)$, $\hat{\sigma}(t) \to f(x,t)$ when $t \to \infty$, where $\varepsilon > 0$, $\hat{x}_1$, $\hat{x}_2$ and $\hat{\sigma}$ are the observer states and $\hat{\sigma}(t) = f(x,t) + o_1$, o_1 is the observation error.

The non-quantized auxiliary control input signals are designed as

$$\bar{\tau} = (-\hat{\sigma} + \dot{\alpha} - c_2\eta_2)/b \tag{12}$$

where c_2 is the normal number.

Step 3: To design the quantized feedback control input τ, in this paper, the error surface and the virtual signal based on the quantized state are defined as

$$\breve{\eta}_1 = Q(x_1) - x_{1d} \tag{13}$$

$$\breve{\eta}_2 = Q(x_2) - \breve{\alpha} \tag{14}$$

$$\breve{\bar{x}}_2 = -c_1\breve{\eta}_1 + \dot{x}_{1d} \tag{15}$$

where the virtual signal $\breve{\bar{x}}_2$ is input into the first-order low-pass filter to obtain the filtered signal $\breve{\alpha}$.

The first-order low-pass filter is defined as

$$\begin{cases} \varsigma\dot{\breve{\alpha}} + \breve{\alpha} = \breve{\bar{x}}_2 \\ \breve{\alpha}(0) = \breve{\bar{x}}_2(0) \end{cases} \tag{16}$$

The ESO is designed as

$$\begin{cases} \dot{\breve{\hat{x}}}_1 = \breve{\hat{x}}_2 + 3\left(Q(x_1) - \breve{\hat{x}}_1\right)/\varepsilon \\ \dot{\breve{\hat{x}}}_2 = \breve{\hat{\sigma}} + b\tau + 3\left(Q(x_1) - \breve{\hat{x}}_1\right)/\varepsilon^2 \\ \dot{\breve{\hat{\sigma}}} = \left(Q(x_1) - \breve{\hat{x}}_1\right)/\varepsilon^3 \end{cases} \tag{17}$$

When $t \to \infty$, it is satisfied that $\breve{\hat{x}}_1 \to Q(x_1)$, $\breve{\hat{x}}_2 \to Q(x_2)$, $\breve{\hat{\sigma}}(t) \to f(x,t)$, where $\varepsilon > 0$, $\breve{\hat{x}}_1$, $\breve{\hat{x}}_2$ and $\breve{\hat{\sigma}}$ are the observer's states and $\breve{\hat{\sigma}}(t) = f(x,t) + o_2$, where o_2 is the observation error.

From Eq. (13) to Eq. (17), the quantized feedback control input τ can be obtained as

$$\tau = (-\breve{\hat{\sigma}} + \dot{\breve{\alpha}} - c_2\breve{\eta}_2)/b \tag{18}$$

2.2 Stability proof

The filtering error generated in the filtering process is defined as

$$\gamma = \alpha - \bar{x}_2 \tag{19}$$

The error surface Eq. (4) and Eq. (5) are derived respectively as

$$\dot{\eta}_1 = \eta_2 + \gamma + \bar{x}_2 - \dot{x}_{1d} = \eta_2 + \gamma - c_1\eta_1 \tag{20}$$

$$\begin{aligned} \dot{\eta}_2 &= f(x,t) + bQ(\tau) - \dot{\alpha} = \\ & b(Q(\tau) - \tau + \tau - \bar{\tau}) + b\bar{\tau} + f(x,t) - \dot{\alpha} = \\ & b(Q(\tau) - \tau) + b(\tau - \bar{\tau}) + o_1 - c_2\eta_2 \end{aligned} \tag{21}$$

where $o_1 = \hat{\sigma} - f(x,t)$.

Lemma 1: Based on a closed-loop system consisting of the controlled object Eq. (2), the low-pass filter Eq. (6) and the control law Eq. (12), the filtering error is bounded.

Proof: The Lyapunov function that defines the filtering error is as follows:

$$\begin{cases} V_\gamma = \gamma\gamma/2 \\ \dot{V}_\gamma = \gamma\dot{\gamma} \end{cases} \tag{22}$$

The filtering error is derived as

$$\dot{\gamma} = -\gamma/\varsigma + c_1\dot{\eta}_1 - \ddot{x}_{1d} \tag{23}$$

From Eq. (6), Eq. (9), and Eq. (19)−Eq. (22), there exists an upper bound function B [23]:

$$\begin{aligned} B &= c_1\dot{\eta}_1 - \ddot{x}_{1d} = c_1(\eta_2 + \gamma + \bar{x}_2 - \dot{x}_{1d}) - \ddot{x}_{1d} = \\ & c_1(\eta_2 + \gamma - c_1\eta_1) - \ddot{x}_{1d} \end{aligned} \tag{24}$$

Therefore,

$$\dot{\gamma} \leqslant -\gamma/\varsigma + B(\eta_1, \eta_2, \gamma, \ddot{x}_{1d}) \tag{25}$$

where the maximum value of B is denoted as M, then $B^2/M^2 - 1 \leqslant 0$.

$$\begin{aligned} \dot{V}_\gamma &\leqslant -\gamma^2/\varsigma + |B||\gamma| \leqslant \left(-1/\varsigma + B^2/2\right)\gamma^2 = \\ & (B^2/M^2 - 1)M^2\gamma^2/2 \leqslant 0 \end{aligned} \tag{26}$$

where $1/\varsigma \geqslant M^2/2 + 1/2$. $\dot{V}_\gamma \leqslant 0$ can be guaranteed when ς is taken sufficiently small. Lemma 1 is proved.

Recursive control design based on Lyapunov stability requires the time derivative of the error surface and the state variables. However, the quantized state variables are discontinuous. Therefore, the Lyapunov-based recursive control design step cannot be used directly. Therefore, to ensure the stability of the closed-loop system, the error between the non-quantized closed-loop signals used in the recursive design step and the quantized feedback tracking control solution presented in Eqs. (13)−(18)

is analyzed (e.g., Lemma 3). For this purpose, the boundedness of the observation errors o_1 and o_2 of the designed ESO is proved by deriving Lemma 2.

For the ESO Eq. (11), it is defined that $\theta = [\theta_1\ \theta_2\ \theta_3]^{\mathrm{T}}$, where

$$\begin{cases}\theta_1 = (x_1 - \hat{x}_1)/\varepsilon^2 \\ \theta_2 = (x_2 - \hat{x}_2)/\varepsilon \\ \theta_3 = f(x,t) - \hat{\sigma} = o_1\end{cases} \tag{27}$$

Because

$$\begin{cases}\varepsilon\dot{\theta}_1(t) = (x_2 - \hat{x}_2 - 3(x_1 - \hat{x}_1)/\varepsilon)/\varepsilon = -3\theta_1 + \theta_2 \\ \varepsilon\dot{\theta}_2(t) = b\bar{\tau} + f(x,t) - \left(b\bar{\tau} + \hat{\sigma} + 3(x_1 - \hat{x}_1)/\varepsilon^2\right) = \\ \qquad -3\theta_1 + \theta_3 \\ \varepsilon\dot{\theta}_3(t) = \varepsilon\left(\dot{f}(x,t) - (x_1 - \hat{x}_1)/\varepsilon^3\right) = -\theta_1 + \varepsilon\dot{f}(x,t)\end{cases} \tag{28}$$

we have the state equation of observer's error as follows:

$$\varepsilon\dot{\boldsymbol{\theta}} = \bar{\boldsymbol{A}}\boldsymbol{\theta} + \varepsilon\bar{\boldsymbol{B}} f(x,t) \tag{29}$$

where

$$\bar{\boldsymbol{A}} = \begin{bmatrix} -3 & 1 & 0 \\ -3 & 0 & 1 \\ -1 & 0 & 0 \end{bmatrix}, \bar{\boldsymbol{B}} = \begin{bmatrix} 0 \\ 0 \\ 1 \end{bmatrix}$$

Hypothesis 3: The unknown term $f(x,t)$ satisfies $\left|\dot{f}(x,t)\right| \leqslant f^*$ where f^* is a positive constant.

The velocity and acceleration of the USV have upper bounds in sailing practice. Therefore, hypothesis 3 is reasonable.

Lemma 2: Under hypothesis 3, for any given symmetric positive definite matrix $\boldsymbol{Q}$, there exists a symmetric positive definite matrix $\boldsymbol{P}$ satisfying the following Lyapunov equation such that the observation error is bounded.

$$\bar{\boldsymbol{A}}^{\mathrm{T}}\boldsymbol{P} + \boldsymbol{P}\bar{\boldsymbol{A}} + \boldsymbol{Q} = 0 \tag{30}$$

Proof: The Lyapunov function of the observer is defined as

$$V_{\mathrm{O}} = \varepsilon\boldsymbol{\theta}^{\mathrm{T}}\boldsymbol{P}\boldsymbol{\theta} \tag{31}$$

Then

$$\begin{aligned}\dot{V}_{\mathrm{O}} &= \varepsilon\dot{\boldsymbol{\theta}}^{\mathrm{T}}\boldsymbol{P}\boldsymbol{\theta} + \varepsilon\boldsymbol{\theta}^{\mathrm{T}}\boldsymbol{P}\dot{\boldsymbol{\theta}} = \\ &\left(\bar{\boldsymbol{A}}\boldsymbol{\theta} + \varepsilon\bar{\boldsymbol{B}}\dot{f}\right)^{\mathrm{T}}\boldsymbol{P}\boldsymbol{\theta} + \boldsymbol{\theta}^{\mathrm{T}}\boldsymbol{P}\left(\bar{\boldsymbol{A}}\boldsymbol{\theta} + \varepsilon\bar{\boldsymbol{B}}\dot{f}\right) = \\ &\boldsymbol{\theta}^{\mathrm{T}}\left(\bar{\boldsymbol{A}}^{\mathrm{T}}\boldsymbol{P} + \boldsymbol{P}\bar{\boldsymbol{A}}^{\mathrm{T}}\right)\boldsymbol{\theta} + 2\varepsilon\boldsymbol{\theta}^{\mathrm{T}}\boldsymbol{P}\bar{\boldsymbol{B}}\dot{f} \leqslant \\ &-\boldsymbol{\theta}^{\mathrm{T}}\boldsymbol{Q}\boldsymbol{\theta} + 2\varepsilon\|\boldsymbol{P}\bar{\boldsymbol{B}}\| + \|\boldsymbol{\theta}\| + \left|\dot{f}\right| \leqslant \\ &-\lambda_{\min}(\boldsymbol{Q})\|\boldsymbol{\theta}\|^2 + 2\varepsilon\|\boldsymbol{P}\bar{\boldsymbol{B}}\|\|\boldsymbol{\theta}\|f^*\end{aligned} \tag{32}$$

where $\lambda_{\min}(\boldsymbol{Q})$ is the smallest eigenvalue of $\boldsymbol{Q}$.

With $\dot{V}_{\mathrm{O}} \leqslant 0$, the convergence condition for the observer can be obtained as

$$\|\boldsymbol{\theta}\| \leqslant 2\varepsilon\left\|\boldsymbol{P}\bar{\boldsymbol{B}}\right\| f^*/\lambda_{\min}(\boldsymbol{Q}) \tag{33}$$

The smaller ε, the faster the convergence of $\boldsymbol{\theta}$. $\|\boldsymbol{\theta}\|$ is $O(\varepsilon)$. As ε decreases, the observation errors o_1 and o_2 converge gradually. Lemma 2 is proved.

Lemma 3: The quantization errors of the error surface, the virtual signal, the filtered signal, the filtering error, and the control input are defined as $\beta_{\eta_1} = \eta - \breve{\eta}_1$, $\beta_{\eta_2} = \eta_2 - \breve{\eta}_2$, $\beta_{\bar{x}_2} = \bar{x}_2 - \breve{\bar{x}}_2$, $\beta_\alpha = \alpha - \breve{\alpha}$, $\beta_{\dot{\alpha}} = \dot{\alpha} - \dot{\breve{\alpha}}$, $\beta_\gamma = \gamma - \breve{\gamma}$, $\beta_\tau = \tau - \bar{\tau}$, respectively.

Suppose that there exist constants $\bar{\beta}_{\eta_1}$, $\bar{\beta}_{\eta_2}$, $\bar{\beta}_{\bar{x}_2}$, $\bar{\beta}_\alpha$, $\bar{\beta}_{\dot{\alpha}}$, $\bar{\beta}_\gamma$, $\bar{\beta}_\tau$, such that $\left|\beta_{\eta_1}\right| \leqslant \bar{\beta}_{\eta_1}$, $\left|\beta_{\eta_2}\right| \leqslant \bar{\beta}_{\eta_2}$, $\left|\beta_{\bar{x}_2}\right| \leqslant \bar{\beta}_{\bar{x}_2}$, $|\beta_\alpha| \leqslant \bar{\beta}_\alpha$, $|\beta_{\dot{\alpha}}| \leqslant \bar{\beta}_{\dot{\alpha}}$, $\left|\beta_\gamma\right| \leqslant \bar{\beta}_\gamma$, $|\beta_\tau| \leqslant \bar{\beta}_\tau$.

Proof:

From Eq. (4) and Eq. (13), $|x_1 - Q(x_1)| \leqslant \chi$, it can be obtained that β_{η_1} is bounded.

$$\left|\beta_{\eta_1}\right| = |x_1 - x_{1d} - (Q(x_1) - x_{1d})| \leqslant \chi = \bar{\beta}_{\eta_1} \tag{34}$$

From Eq. (8) and Eq. (15), we can conclude that $\beta_{\bar{x}_2}$ is bounded.

$$\bar{x}_2 - \breve{\bar{x}}_2 = -c_1\eta_1 + \dot{x}_{1\mathrm{d}} - (-c_1\breve{\eta}_1 + \dot{x}_{1\mathrm{d}}) = -c_1\eta_1 + c_1\breve{\eta}_1 \tag{35}$$

$$\left|\beta_{\bar{x}_2}\right| \leqslant \chi = \bar{\beta}_{\bar{x}_2} \tag{36}$$

From Eq. (19) to Eq. (26), the filtering error is bounded.

$$\left|\beta_\gamma\right| \leqslant \bar{\beta}_\gamma \tag{37}$$

Then β_α is bounded from Eq. (19).

$$\begin{aligned}|\beta_\alpha| &= |\alpha - \breve{\alpha}| = \left|(\gamma + \bar{x}_2) - \left(\breve{\gamma} + \breve{\bar{x}}_2\right)\right| \leqslant \\ &|\gamma - \breve{\gamma}| + \left|\bar{x}_2 - \breve{\bar{x}}_2\right| \leqslant \bar{\beta}_\gamma + \bar{\beta}_{\bar{x}_2} = \bar{\beta}_\alpha\end{aligned} \tag{38}$$

$\beta_{\dot{\alpha}}$ is bounded from the low-pass filter Eq. (6) and Eq. (16).

$$\begin{aligned}|\beta_{\dot{\alpha}}| &= \left|\dot{\alpha} - \dot{\breve{\alpha}}\right| = \left|(\bar{x}_2 - \alpha\varsigma) - \left(\breve{\bar{x}}_2 - \breve{\alpha}\varsigma\right)\right| \leqslant \\ &|\alpha - \breve{\alpha}|\varsigma + \left|\bar{x}_2 - \breve{\bar{x}}_2\right|\varsigma \leqslant \bar{\beta}_\alpha + \bar{\beta}_{\bar{x}_2}\varsigma = \bar{\beta}_{\dot{\alpha}}\end{aligned} \tag{39}$$

From Eq. (5) and Eq. (14), $|x_2 - Q(x_2)| \leqslant \chi$. Then β_{η_2} is bounded.

$$\left|\beta_{\eta_2}\right| = |(x_2 - Q(x_2)) - (\alpha - \breve{\alpha})| \leqslant \chi + \bar{\beta}_\alpha = \bar{\beta}_{z_2} \tag{40}$$

From Eq. (12) and Eq. (18), β_τ is bounded:

$$\begin{aligned}\beta_\tau &= \left(-\breve{\hat{\sigma}} + \dot{\breve{\alpha}} - c_2\breve{\eta}_2 + \hat{\sigma} - \dot{\alpha} + c_2\eta_2\right)/b = \\ &(f(x,t) + o_2 - f(x,t) - o_1)/b - \\ &(\dot{\breve{\alpha}} - \dot{\alpha} + c_2(\eta_2 - \breve{\eta}_2))/b\end{aligned} \tag{41}$$

$$|\beta_\tau| \leqslant \left(|o_1| + |o_2| + \bar{\beta}_{\dot{\alpha}} + c_2\bar{\beta}_{\eta_2}\right)\Big/ b = \bar{\beta}_\tau \tag{42}$$

Lemma 3 is proved.

Based on the heading tracking, the virtual control and the filtering error, the Lyapunov function is defined as

$$V_{\mathrm{S}} = {\eta_1}^2/2 + {\eta_2}^2/2 + \gamma^2/2 \tag{43}$$

Theorem 1: Based on the quantized closed-loop system, if $V_S(0) \leqslant p$ and $p>0$, the closed-loop system error signal is consistent and eventually bounded.

Proof: When $V_{\mathrm{S}} = p$, there must have

$$\begin{aligned}\dot{V}_{\mathrm{S}} &= \eta_1(\eta_2 + \gamma) - c_1{\eta_1}^2 - c_2{\eta_2}^2 + \gamma(-\gamma/\varsigma + B) + \\ &\eta_2(b(Q(\tau) - \tau) + b(\tau - \bar{\tau}) + o_1) \leqslant \\ &|\eta_1||\eta_2| + |\eta_1||\gamma| - c_1{\eta_1}^2 - c_2{\eta_2}^2 - \gamma^2/\varsigma + |\gamma||B| + \\ &|\eta_2|(b|Q(\tau) - \tau| + b|\tau - \bar{\tau}| + o_1) \leqslant\end{aligned}$$

$$\left(\eta_1{}^2+\eta_2{}^2\right)/2+\left(\eta_1{}^2+\gamma^2\right)/2-c_1\eta_1{}^2-c_2\eta_2{}^2-$$
$$\gamma^2/\varsigma+\gamma^2B^2/2+\left(3\eta_2{}^2+b^2\chi^2+b^2\bar{\beta}_\tau{}^2+o_1\right)/2=$$
$$(1-c_1)\eta_1{}^2+(2-c_2)\eta_2{}^2+(B^2/2-1/\varsigma+1/2)\gamma^2+$$
$$1/2+\left(b^2\chi^2+b^2\bar{\beta}_\tau{}^2+o_1\right)/2 \tag{44}$$

in which, $c_1\geqslant 1+\Omega_2$, $c_2\geqslant 2+\Omega_2$, $\Omega_2>0$, $1/\varsigma\geqslant M^2/2+1/2+\Omega_2$, $\varDelta=\left(b^2\chi^2+b^2\beta_\tau{}^2+\varLambda\right)/2$, $o_1<\varLambda$.

Therefore, we have

$$\dot{V}_{\rm S}\leqslant-\Omega_2|\eta_1|^2-\Omega_2|\eta_2|^2+$$
$$(-M^2/2+B^2/2-\Omega_2)\gamma^2+\varDelta=$$
$$-2\Omega_2p+(B^2/M^2-1)M^2\gamma^2/2+\varDelta\leqslant-2\Omega_2p+\varDelta \tag{45}$$

Considering the system in a comprehensive manner, we have

$$\dot{V}=\dot{V}_{\rm S}+\dot{V}_{\rm O}\leqslant-2\Omega_2p+\varDelta-\lambda_{\min}(\boldsymbol{Q})\|\boldsymbol{\theta}\|^2+2\varepsilon f^*\|\boldsymbol{P}\bar{\boldsymbol{B}}\|+\|\boldsymbol{\theta}\| \tag{46}$$

When Ω_2 is taken large enough and ε is taken small enough, $\dot{V}\leqslant 0$ is guaranteed. Therefore, the closed-loop system error signal is consistent and eventually bounded. The convergence speed depends on Ω_2 and the observer parameter ε.

3 Simulation results

Taking the USV "Blue Letter" of Dalian Maritime University as an example, the parameters are selected as follows: a length of 7.02 m, a width of 2.6 m, load draught of 0.32 m, a block coefficient of 0.697 6, and a speed of 35 kn. As a result, the ship model parameters are calculated as follows [24]: K = 0.71, T = 0.32, b = K/T = 2.2. The nonlinearity coefficient of Norrbin motion model a = 0.001 is selected.

In simulation scenario 1, the desired heading command is set as $x_{1\rm d}$ = 5sin(t/10). The initial state of the actual controlled object is [5, 2]. By combining the time-varying parameter trajectory and the characteristics of the physical parameters of the USV, the quantization level is selected as χ = 0.002. The parameter c_1 = 1.5 is selected according to Eq. (15). The time constant ς = 0.01 of the low-pass filter is selected according to Eq. (16). The expansion observer parameter ε=0.01 is selected according to Eq. (17). The parameter c_2=2 is selected according to Eq. (18). The simulation results obtained are shown in Figs. 2−5.

Figs. 2−5 show the heading tracking results, tracking errors, ESO observations and control inputs before and after quantization in simulation scenario 1, respectively. Fig. 2 shows the tracking results of a ship's heading angle and a ship's yaw rate. Fig. 3 shows a ship's heading angle error $Q(x_1)-x_{1\rm d}$ and the yaw rate error $Q(x_2)-x_{2\rm d}$. According to the simulation results, it can be seen that the designed controller is effective in controlling a ship and can track the heading well. The errors can converge to a small residual set quickly. Fig. 4 shows the observation results of the ESO. The function estimation curve of the ESO can quickly coincide with the original function curve. The observation effect is ideal. Fig. 5 shows the control inputs τ and $Q(\tau)$ before and after quantization. According to the

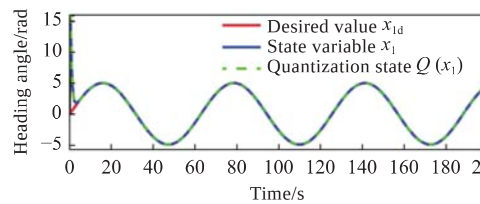

(a) Tracking results of heading angle

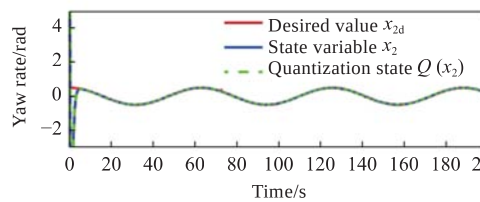

(b) Tracking results of yaw rate

Fig. 2 Ship tracking results of heading angle and yaw rate

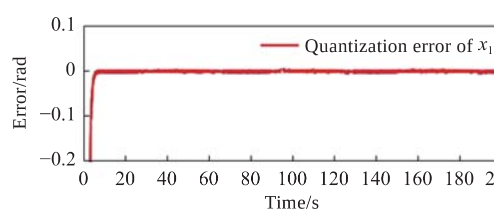

(a) Heading angle error

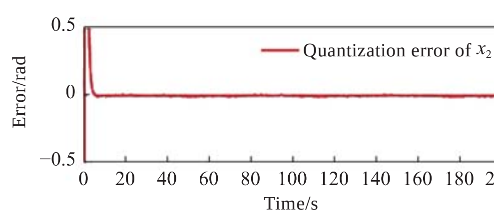

(b) Yaw rate error

Fig. 3 Ship heading angle error and yaw rate error

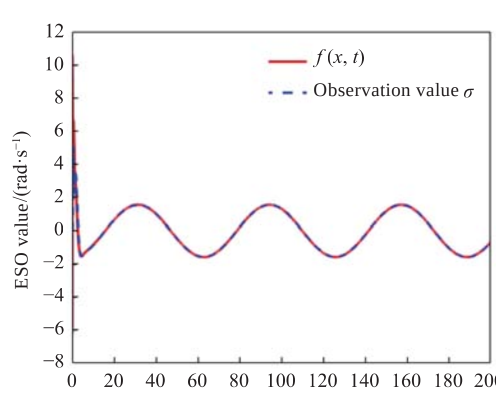

Fig. 4 Observation results of ESO

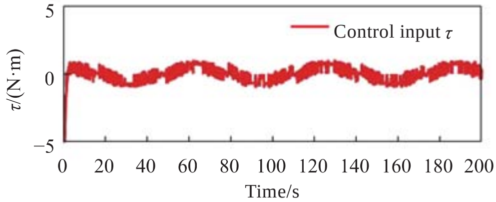

(a) Control input before quantization

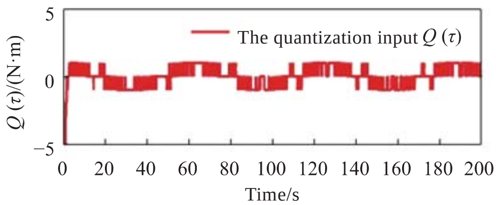

(b) Control input after quantization

Fig. 5 Control inputs before and after quantization

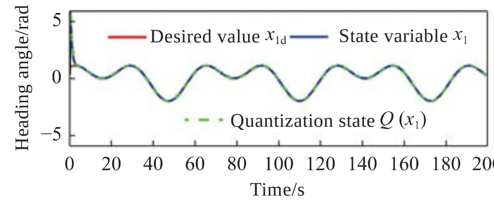

(a) Tracking results of heading angle

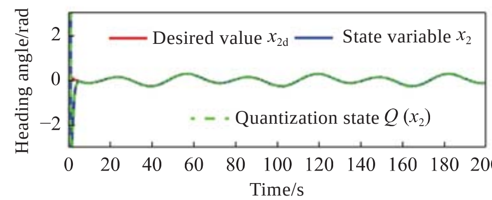

(b) Tracking results of yaw rate

Fig. 6 Ship tracking results of heading angle and yaw rate

simulation results, the controller is considered to perform one operation when the control input is set to change by 0.01 N·m every time. When the control input is not quantized, the controller executes 11 854 times. After the control input is quantized, the controller executes 1 463 times. According to the comparison results, the quantization process reduces the execution frequency of the controller and decreases the rudder amplitude, which can effectively reduce the burden of signal transmission in a network.

To further verify the rationality and applicability of the control strategy designed in this paper, in simulation scenario 2, the desired heading command $x_{1d}=\sin(t/10)+\cos(t/5)$ is set, and the physical parameters, initial state and other controller parameters of USV are the same as those in simulation scenario 1. The simulation results are shown in Figs. 6–9.

Figs. 6–9 show the heading tracking results, tracking errors, ESO observation results and control inputs before and after quantization in simulation scenario 2, respectively. According to the simulation results, it can be seen that the controller can track the heading well in simulation scenario 2. The error can be converged to a small residual set quickly. The ESO observation results are satisfactory. According to the results, when the controller is set to execute once for every 0.01 N·m change in the control input, the controller executes 14 437 times when the control input is not quantized, and 1 965 times when the control input is quantized. According to the comparison results, the quantization process reduces the burden of signal transmission in the network. The simulation results further verify that the control quality of heading tracking is not significantly sacrificed by considering state quantization and input quantization issues in the control system.

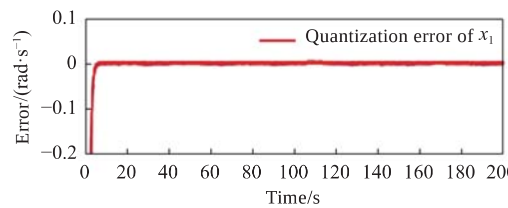

(a) Heading angle error

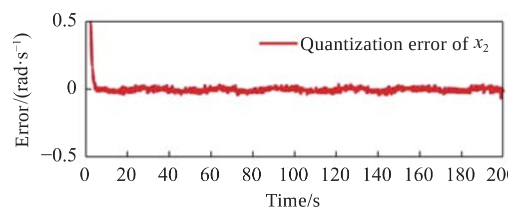

(b) Yaw rate error

Fig. 7 Ship heading angle error and yaw rate error

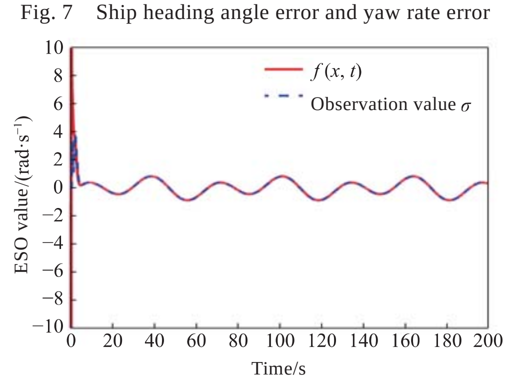

Fig. 8 Observation results of ESO

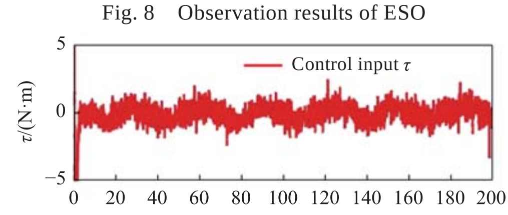

(a) Control input before quantization

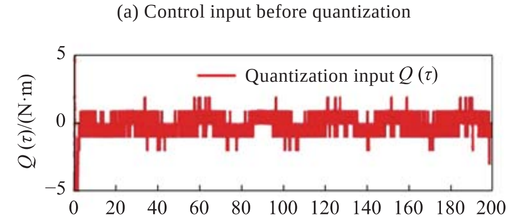

(b) Control input after quantization

Fig. 9 Control inputs before and after quantization

4 Conclusion

In this paper, considering the practical problem of limited communication bandwidth in nautical practice, an ESO-based quantized feedback tracking control method is investigated for USVs with state quantization and input quantization, which reduces the burden of signal transmission, reduces the execution frequency of an executor, and is more in line with the control law of multistage servo systems in nautical practice. The ESO-based quantized feedback tracking controller is designed to ensure that the USV tracks the desired heading, and at the same time realizes the estimation of unknown perturbations and system uncertainties. The systematic and generalized methods for quantization error consideration and closed-loop system stability determination proposed in this paper rigorously demonstrate the stability of the designed USV heading tracking control system with state quantization and input quantization. Simulation experiments verify the effectiveness of the control strategy proposed in this paper.

References

[1] GAO P, WAN L, XU Y F, et al. Point stabilization control of benthic AUV based on fixed-time extended state observer [J]. Chinese Journal of Ship Research, 2022, 17 (4): 71−78 (in Chinese).

[2] YI G, LIU Z, ZHANG J Q, et al. A USV heading tracking control method based on improved terminal sliding mode control [J]. Electronics Optics & Control, 2020, 27 (10): 12−16, 21 (in Chinese).

[3] NING J, CHEN H M, LI W, et al. Finite-time ship formation control based on extended state observer [J]. Chinese Journal of Ship Research, 2023, 18 (1): 60−66 (in Chinese).

[4] WU Q M, CHEN Z B. Application of model reference neural network algorithm in ship course control [J]. Ship Science and Technology, 2020, 42 (22): 10−12 (in Chinese).

[5] MA S F, ZHANG W J, YIN J C, et al. RBF-network-based predictive ship course control [C]//2020 Chinese Control and Decision Conference (CCDC). Hefei: IEEE, 2020: 3506−3511.

[6] AN S, HE Y, WANG L J. A ship course control approach based on backstepping adaptive algorithm [J]. Mechanical and Electrical Equipment, 2020, 37 (6): 65−69,

[7] HAN L J. Design of ship heading control system based on neural network algorithms [C]//Proceedings of the 5th International Conference on Intelligent Education and Artificial Intelligence Development in 2022. Beijing: Hong Kong New Century Culture Publishing House, 2022: 21−23. (in Chinese).

[8] LI G J, LI C X, YI Z R. Event-triggered logic switch adaptive control for course keeping [J]. Ship Science and Technology, 2022, 44 (11): 76−81 (in Chinese).

[9] CHU R T, LIU Z Q. Ship course sliding mode control system based on FTESO and sideslip angle compensation [J]. Chinese Journal of Ship Research, 2022, 17 (1): 71−79 (in Chinese).

[10] WANG W X, LIU S, ZHANG G Q, et al. Robust adaptive course-keeping control of under-actuated ships with the rudder failure [J]. Chinese Journal of Ship Research, 2023, 18 (1): 116−123 (in Chinese).

[11] ZHOU J, WEN C Y, YANG G H. Adaptive backstepping stabilization of nonlinear uncertain systems with quantized input signal [J]. IEEE Transactions on Automatic Control, 2014, 59 (2): 460−464.

[12] LIU W H. Adaptive control and sampled-data control for nonlinear systems with input quantization [D]. Nanjing: Nanjing University of Science and Technology, 2017 (in Chinese).

[13] QI X J, LIU W H. Adaptive finite-time dynamic surface control for nonlinear systems with input quantization and unknown disturbances [J]. Journal of Nanjing University of Information Science Technology (Natural Science Edition),2020,12 (3):330−340 (in Chinese).

[14] WU J, SUN W, SU S F, et al. Adaptive asymptotic tracking control for input-quantized nonlinear systems with multiple unknown control directions[J/OL]. IEEE Transactions on Cybernetics, 2022: 1−10 (2022-07-12) [2023-04-10]. https://ieeexplore. ieee. org/document/ 9827984.

[15] ZHOU J, WEN C Y, WANG W, et al. Adaptive backstepping control of nonlinear uncertain systems with quantized states [J]. IEEE Transactions on Automatic Control, 2019, 64 (11): 4756−4763.

[16] KIM B M, YOO S J. Adaptive neural control of uncertain MIMO nonlinear pure-feedback systems via quantized state feedback [J]. IEEE Access, 2022, 10: 38729−38741.

[17] YANG W Q, ZHOU S Y, LU J H, et al. Research on fault tolerant control technology of carrier aircraft based on ESO compensation [J]. Electronics Optics & Control, 2023, 30 (7): 28−34, 56 (in Chinese).

[18] LI J, LI G Y. Path planning and tracking control based on improved artificial potential field [J]. Journal of Chongqing Jiaotong University (Natural Science), 2020, 39 (9): 25−30, 37 (in Chinese).

[19] ZHENG B C, YANG G H. Quantized output feedback stabilization of uncertain systems with input nonlinearities via sliding mode control [J]. International Journal of Robust and Nonlinear Control,2014,24(2):228−246.

[20] PENG Z H, WANG D, LI T S, et al. Output-feedback cooperative formation maneuvering of autonomous surface vehicles with connectivity preservation and collision avoidance [J]. IEEE Transactions on Cybernetics, 2020, 50 (6): 2527−2535.

[21] PARAVISI M, SANTOS D H, JORGE V, et al. Un-

manned surface vehicle simulator with realistic environmental disturbances [J]. Sensors,2019,19 (5): 1068.
[22] BROCKETT R W, LIBERZON D. Quantized feedback stabilization of linear systems [J]. IEEE Transactions on Automatic Control, 2000, 45 (7): 1279−1289.
[23] FARRELL J A, POLYCARPOU M, SHARMA M, et al. Command filtered backstepping [J]. IEEE Transactions on Automatic Control, 2009, 54 (6): 1391−1395.
[24] XIANG L K, LI X, JIANG Y, et al. Model identification of unmanned surface vehicle propulsion system [J]. Chinese Journal of Ship Research, 2019, 14 (Supp 1): 7 −11, 22 (in Chinese).

带有状态/输入量化的无人艇航向跟踪控制

李伟[1], 王雨[1], 宁君*[1], 李志慧[2]
1 大连海事大学 航海学院, 辽宁 大连 116026
2 吉林师范大学 信息技术学院, 吉林 四平 136000

摘　要: [**目的**] 针对水面无人艇(USV)的海上通信受限的问题,提出一种带有状态/输入量化的USV航向跟踪控制方法。[**方法**] 基于反步法设计系统控制律,结合动态面技术降低虚拟控制律的计算量膨胀问题。对于控制系统中存在的不确定项及外界干扰,利用扩张状态观测器(ESO)进行估计。采用均匀量化器分别对控制系统中的状态变量和控制输入进行量化,且量化后的状态反馈信息仅用于跟踪控制。利用量化状态递归设计基于ESO的USV航向控制器,证明闭环控制系统中量化变量和非量化变量间误差的有界性。[**结果**] 基于李雅普诺夫稳定性理论,提出了量化误差考量及闭环系统稳定性判定方法,严格证明了所设计的带有状态量化和输入量化的USV航向跟踪控制系统的稳定性,仿真实验验证了该控制策略的有效性。[**结论**] 结果表明,所提方法可为USV航向跟踪控制提供借鉴。

关键词: 无人艇; 状态量化和输入量化; 量化反馈控制; 扩张状态观测器; 量化误差